

Quantifying Magnetic Domain Correlations in Multilayer Films

Y. U. Idzerda, V. Chakarian, and J. W. Freeland*

Naval Research Laboratory, Washington, D.C. 20375

(Received 20 July 1998)

The vertical correlation of magnetic domains in a Co/Cr/Co trilayer is statistically quantified as a function of an applied magnetic field. These measurements, used with determinations of the individual layer magnetometry curves, identify the presence of both antiferromagnetic exchange coupling and ferromagnetic dipolar coupling for different regions within the trilayer. [S0031-9007(99)08427-6]

PACS numbers: 75.70.Cn, 75.25.+z, 75.60.Ej

With the explosive growth [1–4] in spin-polarized electron transport studies for spin-tunneling [5,6], spin-transistor [7], and magnetoresistive [8–10] device applications, the importance of the correlation in the orientations of magnetic domains is becoming increasingly apparent. The spin conductance of a magnetic heterostructure is controlled by the relative orientation of the magnetic moment directions of the component layers on a local scale (within a few spin mean-free paths) [11]. In real systems, local variations of the film and interface microstructure alter the interlayer and intralayer coupling energies and therefore the field dependence of the relative orientation of the layer magnetic moments. Any meaningful comparison between the measured and calculated spin conductances requires a quantitative description of the field dependence of the magnetic domain correlations. Furthermore, the determination of the local domain alignments can be used to identify, and quantify, the possible interlayer and intralayer coupling mechanisms present in these films, as well as elucidate modifications of magnetic behavior from film lithography and device manufacture.

Magnetic domain structure of a multilayer on this appropriate length scale can be obtained by magnetic microscopy, in its many and varied forms [12], but the magnetic mapping is typically averaged by a depth weighting factor and does not isolate the relative moment directions of the component layers. One exception is magnetic imaging employing magnetic circular dichroism (MCD) [13]. (Magneto-optic techniques [14] also have this capability with spatial resolution but for very particular systems.) Magnetic circular dichroism is a powerful magnetic structure characterization tool and has been used for the determination of element-specific magnetometry [15] and vector magnetometry [16] information, even identifying the hysteretic behavior of an ultrathin buried magnetic layer sandwiched between two large ferromagnetic sheets [17].

A statistical mapping of the correlations between magnetic domains in different layers can be generated by MCD imaging, but this is a laborious and lengthy task which is difficult to perform in the presence of a significant applied field (with the notable exception of MCD transmission [18] and magneto-optical [14] microscopy). Instead, the correlation between magnetic domains can be statis-

tically quantified by measuring the magnetic field dependence of the x-ray resonance magnetic scattering (XRMS) [19–22]. X-ray resonance magnetic scattering is the angle dependent specular reflectance of circular polarized soft x rays whose energy is tuned to the absorption energy of a magnetic element. It combines the element selectivity of x-ray resonant scattering with the magnetic contrast of magnetic circular dichroism, and has been successfully used to extract chemical and magnetic film thicknesses with 0.05 Å sensitivity [23], identify the order of layer switching, and separately parametrize the magnetic and chemical roughness of interfaces [23–25].

The specular scattered intensity of a resonant soft x ray is a function of the incident angle of the soft x-ray θ and the magnetic configuration of the multilayer (which is dependent on the applied magnetic field history). For a single film with magnetic domains large compared to the photon coherence length, the reflected intensity $I(\theta, B)$ is given by

$$I(\theta, B) = \sum_k I_k(\theta)x_k(B), \quad (1a)$$

where k denotes a particular magnetic domain type within the film, I_k is the scattered intensity from that domain, and x_k is the fraction of the film in the k th domain type. (Note that $\sum_k x_k(B) = 1$ at any field value.) For a film which exhibits a uniaxial magnetic anisotropy and therefore has predominantly two possible magnetic domains (left and right), Eq. (1a) becomes

$$I(\theta, B) = I^{\rightarrow}(\theta)x^{\rightarrow}(B) + I^{\leftarrow}(\theta)x^{\leftarrow}(B). \quad (1b)$$

Equation (1a) can also apply to a multilayer film, but now k denotes a particular configuration of the magnetic moment orientations for each magnetic layer taken vertically along the multilayer. I_k is the scattered intensity from that moment configuration and x_k is the fraction of the multilayer in that particular configuration [26]. Similarly, extending Eq. (1b) to a magnetic film system consisting of two layers, each with two possible magnetic domain directions, the total scattered intensity becomes

$$I(\theta, B) = I^{\rightarrow}x^{\rightarrow\rightarrow} + I^{\rightarrow}x^{\rightarrow\leftarrow} + I^{\leftarrow}x^{\leftarrow\rightarrow} + I^{\leftarrow}x^{\leftarrow\leftarrow}, \quad (2)$$

where $x^{\rightarrow\rightarrow}$ and $x^{\leftarrow\leftarrow}$ are the fractions of the film with the magnetic domains of the top and bottom film aligned

with each other and x^{\rightleftharpoons} and x^{\leftarrow} are the fractions of the film antialigned to each other. It is these four magnetic field dependent fractions which will ultimately express the vertical correlation of magnetic domains in the trilayer, and it is the extraction of these terms from the measured scattered intensities which is the subject of this Letter.

To experimentally realize only these four magnetic domain configurations, a magnetic structure with a strong uniaxial magnetic anisotropy is utilized. To accomplish this, a single crystal Co(50 Å)/Cr(35 Å)/Co(50 Å) trilayer is deposited at 175 °C at a vacuum of $<5 \times 10^{-10}$ Torr, on an epitaxially grown ZnSe(001) substrate (shown in Fig. 1). To stabilize the bcc Co structure, a seed layer of 5 Å of bcc Fe is first deposited on the ZnSe. The growth of the second Co layer on the bcc Cr also produces a single crystal bcc structure [27,28]. The multilayer is then capped with a 30-Å Al layer to prevent oxidation.

Vibrating sample magnetometry (VSM) confirmed that this system displayed a strong uniaxial anisotropy, superimposed on the cubic magnetic anisotropy inherent to the fourfold surface and identified the easy-easy axis of magnetization to be in the [110] direction. Magnetic force microscopy (MFM) measurements taken for the trilayer showed only two magnetic domain configurations, with the net magnetization direction along the [110] axis. The MFM measurement could not isolate the moment direction of each individual Co layer but, as previously noted, represents some depth-weighted average of the entire magnetic structure.

As shown in Fig. 1, the soft x ray is incident at an angle θ , and the specular reflected intensity is measured using a Si photodiode located at an angle 2θ to the incident beam direction (θ to the film plane). The circular polarized soft x ray (degree of polarization is set to 75%) is tuned to the Co L_3 edge (778 eV), corresponding to the maximum in the Co absorption curve (imaginary part of the complex Co dielectric tensor).

To quantify the magnetic domain configuration fractions $x_k(B)$, the applied field dependence of the scattered intensity is measured. But, as indicated in Eq. (1a), the contributions to the total scattered intensity depend separately on the applied magnetic field and on the incidence angle.

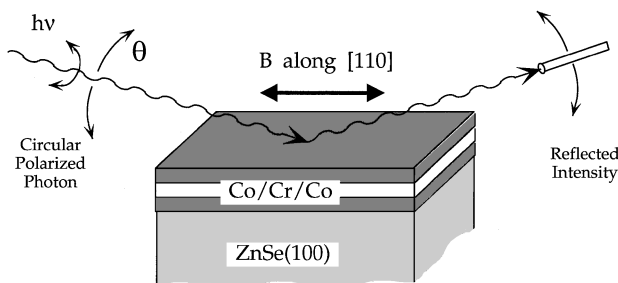


FIG. 1. XRMS scattering geometry for a Co/Cr/Co single crystal trilayer with the field applied along the magnetically easy-easy [110] axis.

This latter angular dependence is demonstrated in the top panel of Fig. 2, where the log of the specular scattered intensities for negative helicity light and the resulting asymmetry $(I^+ - I^-)/(I^+ + I^-)$ are shown for the sample fully magnetized by an applied field of +120 Oe (I^+) and -120 Oe (I^-). Displayed with these angle dependent reflectance curves is a subset of the field dependent reflected intensity curves recorded at the reported incidence angles (shown in the eight curves at the bottom of Fig. 2). Because of the changing contribution of the scattering intensities $I_k(\theta)$, these curves are markedly different.

The obvious variation in these curves belies a hidden similarity. In Eq. (2), the dependence on the applied magnetic field is contained only in the four configuration fractions $x_k(B)$, whereas the angular dependence is derived solely from the four prefactor terms $I^{\rightleftharpoons}(\theta)$, $I^{\leftarrow}(\theta)$, $I^{\rightleftharpoons}(\theta)$, and $I^{\leftarrow}(\theta)$ which each remain constant for a fixed incident angle. The large variations observed in the field scans taken at different incidence angles (Fig. 2) result only from a variation of these multiplicative constants and allow for a separate determination of the four configuration fractions $x^{\rightleftharpoons}(B)$, $x^{\leftarrow}(B)$, $x^{\rightleftharpoons}(B)$, and $x^{\leftarrow}(B)$ which are independent of the incidence angle.

Actually, only two of these prefactors are unknown. In the top panel of Fig. 2, we show the experimentally

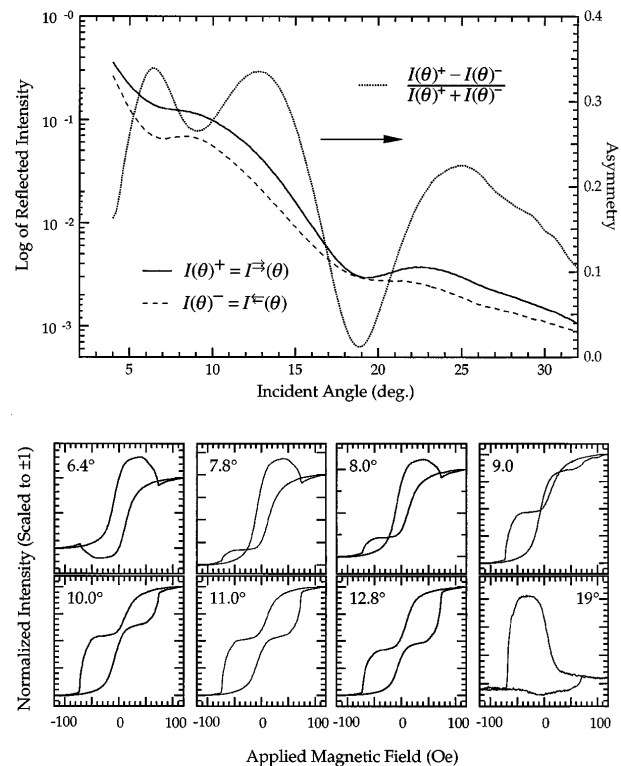


FIG. 2. Top panel: Scattered intensity and a normalized asymmetry for circular polarized soft x rays near the Co L_3 edge (778 eV) for a trilayer fully magnetized in either direction. Bottom panel: Eight magnetic field dependent specular intensity spectra acquired at the indicated incidence angle for circular polarized soft x rays near the Co L_3 edge (778 eV).

determined values for the angle dependence of the scattered intensity when the film is completely magnetized to saturation in the positive [$x^{\rightarrow} = 1$ and $I^+(\theta) = I^{\rightarrow}(\theta)$] or negative [$x^{\leftarrow} = 1$ and $I^-(\theta) = I^{\leftarrow}(\theta)$] field direction. Utilizing the many field dependent scans, an iterative, least-squares, best-fit procedure can be applied to determine the two remaining unknown intensity factors, which are different constants for each scan, and the four configuration fractions, which must be the same for *all* scans. In this way, the fraction of the film with a particular magnetic domain configuration can be uniquely determined.

The validity of this procedure can be checked by comparing measured magnetometry loops with calculated magnetometry loops derived from the four extracted domain configuration fractions by noting that the moment of the bottom layer, M_{bottom} , is given by

$$M_{\text{bottom}} = M_0(x_1^{\rightarrow} - x_1^{\leftarrow}), \quad (3)$$

where x_1^{\rightarrow} (x_1^{\leftarrow}) is the fraction of the bottom magnetic layer with moment along (opposed to) the applied field direction. This can be rewritten in terms of the four configuration fractions by noting that $x_1^{\rightarrow} = x^{\rightarrow\rightarrow} + x^{\leftarrow\rightarrow}$ and $x_1^{\leftarrow} = x^{\rightarrow\leftarrow} + x^{\leftarrow\leftarrow}$ (and similarly for the top magnetic layer).

The top panel of Fig. 3 shows both the normalized total moment hysteresis curve (measured by vibrating sample magnetometry) as well as the normalized hysteresis curve of just the bottom layer. We have directly measured the hysteresis behavior of the bottom film by measuring the element-specific hysteresis curve in absorption of the strongly coupled Fe seed layer used as a template to es-

tablish the bcc growth of Co. (Element-specific magnetic hysteresis measurements of a single 50-Å Co layer deposited on a 5-Å Fe seed layer showed the Fe and Co hysteretic behavior to be identical.) Superimposed over these curves are the calculated hysteresis loops as determined from the four extracted configuration fractions and Eq. (3). The agreement is nearly exact, giving confidence in the extraction of the film fractions.

Rather than display the four configuration fractions separately, a more meaningful and compact presentation is plotted in the bottom panel of Fig. 3. For spin-conductance applications, it is the relative orientation of the magnetic moments within a domain which gives rise to the resistance variation (aligned for low resistance, antialigned for high resistance). Therefore, the correlation function ($x^{\uparrow\uparrow} - x^{\uparrow\downarrow}$) representing the fraction of the film which is aligned, $x^{\uparrow\uparrow} = x^{\rightarrow\rightarrow} + x^{\leftarrow\leftarrow}$, minus the fraction of the film antialigned, $x^{\uparrow\downarrow} = x^{\rightarrow\leftarrow} + x^{\leftarrow\rightarrow}$, is a more useful quantity to examine. This quantity is simply the average deviation from ferromagnetic-type alignment of the magnetization of the two layers, where a value of +1 (−1) represents complete alignment (antialignment) of the two film moments.

At high fields, the two Co films are aligned with each other and both essentially single magnetic domains. As the field is increased or decreased from these extremes, domains form (first in the top Co film) and the correlation function is reduced from unity. The correlation function drops to a minimum value and returns to unity at the opposite extreme. From Fig. 3, it is clear that the Co/Cr/Co film never reaches a fully antialigned configuration, but achieves a maximum negative value of −55%. This field value corresponds to the peak in the magnetoresistance since it is at this point that the two magnetic layers are most antialigned and the trilayer has the highest resistance. This correlation function can be used in conjunction with measured transport curves to extract the coefficient of magnetoresistance [29] or for a detailed comparison with theory. It can also be used to identify and quantify the interlayer coupling mechanisms present in this multilayer.

In the absence of any type of interactions between the magnetic layers, the purely random distribution of magnetic domains will still result in a statistical probability that two vertically offset regions of different magnetic layers within the multilayer are aligned with each other. For two noninteracting independent films, the predicted fraction of the film in a particular configuration, $X_{N1}(B)$, can be calculated as simply the product of the individual domain fractions of each layer (i.e., keeping with the previous notation $x_{N1}^{\rightarrow\rightarrow} = x_1^{\rightarrow} \times x_2^{\rightarrow}$, and similarly for each of the other configurations). Since, as shown in Fig. 3, the individual layer fractions can be extracted from either the magnetometry data or the measured two-layer configuration fractions themselves, a correlation function for two noninteracting films can be separately constructed for comparison with the derived correlation function of Fig. 3. By comparing the calculated noninteracting films

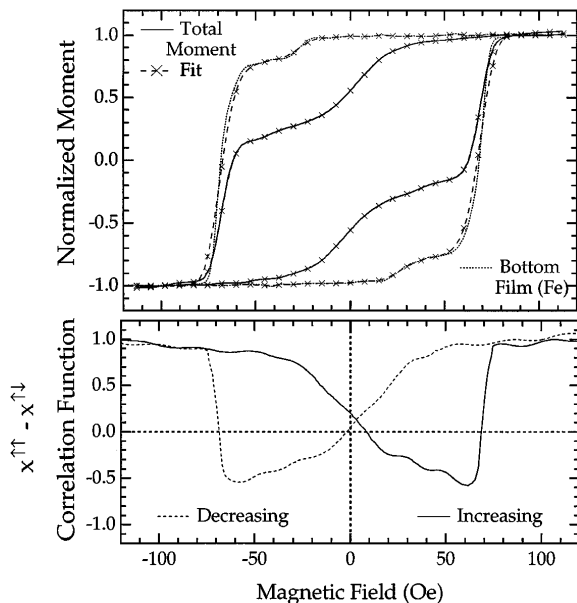


FIG. 3. Top panel: Normalized magnetometry loops for the total moment and only the bottom film (the Fe hysteresis loop). Superimposed is the calculated hysteresis loops from the configuration fractions (see text). Bottom panel: The extracted correlation function (as defined in the text) for increasing and decreasing field.

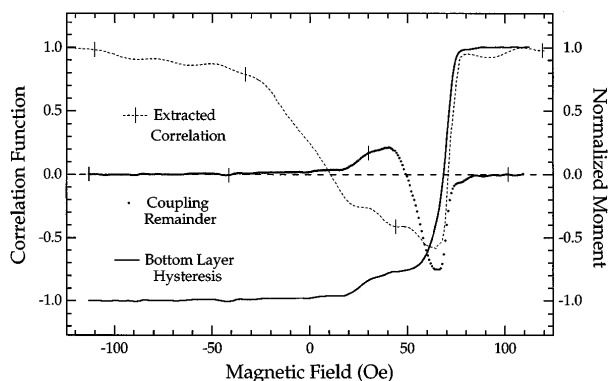


FIG. 4. The bottom layer hysteresis behavior (solid line), the extracted correlation function (dashed line), and the coupling-derived remainder of the correlation function (dots) of the Co/Cr/Co trilayer as a function of increasing field.

correlation function to the extracted correlation function, we can imply the presence of coupling between the magnetic layers and even ascertain the sign of the coupling.

This comparison is performed in Fig. 4, where is shown the bottom film hysteresis curve, the extracted correlation function, and the difference between the extracted correlation function and the calculated correlation function for noninteracting films, each for only the increasing field leg of the hysteresis loop. This difference is just the remainder of the correlation function caused by coupling between the films [30]. As the field is increased in the data of Fig. 4, the extracted correlation function is reduced while the bottom film hysteresis loop shows that the bottom film is still near saturation. Since the coupling-derived remainder of the correlation function remains zero, as it must if either film is at saturation, the initial reduction in the extracted correlation function would occur regardless of the presence or absence of any interaction between the films. As the field is increased farther, the coupling-derived remainder of the correlation function remains near zero until a significant number of magnetic domains have begun to form in the bottom film. At this point, the coupling-derived remainder of the correlation function becomes nonzero and positive, indicating that a significant fraction of the film is interacting and that the magnetic domains are preferentially aligned to those domains directly opposite them in the adjacent layer, probably from dipolar coupling. At higher applied fields, this predominant ferromagnetic interaction is replaced by an antiferromagnetic coupling, indicating that the majority of the sample is now dominated by an antiferromagnetic interlayer coupling mechanism.

Of the various formulations for describing the magnetic domains with this trilayer system, it is the final coupling-

derived remainder of the correlation function associated with interacting films which probes the fundamentally significant behavior of the magnetic films by identifying and quantifying the type and strength of the interlayer coupling mechanisms. Although the correlation function and the two-layer domain configuration fractions themselves are tremendously useful for understanding spin-transport behavior, the coupling-derived remainder of the correlation function provides the physical insight, and becomes even more useful when investigating coupling mechanisms as functions of changing temperature, interlayer thickness, or after film lithography and device processing.

This work was supported by the Office of Naval Research. NSLS is supported by DOE.

*Permanent address: Adv. Photon Source, Argonne, IL 60439.

- [1] G. A. Prinz, *Phys. Today* **48**, 58 (1995).
- [2] G. A. Prinz, *Science* **250**, 1092 (1990).
- [3] L. M. Falicov *et al.*, *J. Mater. Res.* **5**, 1299 (1990).
- [4] B. Heinrich and J. F. Cochran, *Adv. Phys.* **42**, 523 (1993).
- [5] R. Meservey *et al.*, *Phys. Rev. Lett.* **25**, 1270 (1970).
- [6] P. M. Tedrow and R. Meservey, *Phys. Rev. B* **7**, 318 (1973).
- [7] D. J. Monsma *et al.*, *Phys. Rev. Lett.* **74**, 5260 (1995).
- [8] P. Grunberg *et al.*, *Phys. Rev. Lett.* **57**, 2442 (1986).
- [9] M. N. Baibich *et al.*, *Phys. Rev. Lett.* **61**, 2472 (1988).
- [10] B. Dieny *et al.*, *Phys. Rev. B* **43**, 1297 (1991).
- [11] P. Bruno and C. Chappert, *Phys. Rev. Lett.* **67**, 1602 (1991).
- [12] P. Grutter *et al.*, in *Scanning Tunneling Microscopy*, edited by R. Weisendanger and H.-J. Guntherodt (Springer, Berlin, 1992), Vol. II, p. 151.
- [13] J. Stohr *et al.*, *Science* **259**, 658 (1993).
- [14] M. Ruhrig *et al.*, *Phys. Status Solidi (a)* **125**, 635 (1991).
- [15] C. T. Chen *et al.*, *Phys. Rev. B* **48**, 642 (1993).
- [16] V. Chakarian *et al.*, *Appl. Phys. Lett.* **66**, 3368 (1995).
- [17] V. Chakarian *et al.*, *Phys. Rev. B* **53**, 11 313 (1996).
- [18] P. Fischer *et al.*, *J. Phys. D* **31**, 645 (1998).
- [19] K. Namikawa *et al.*, *J. Phys. Soc. Jpn.* **54**, 4099 (1985).
- [20] C.-C. Kao *et al.*, *Phys. Rev. B* **50**, 9599 (1994).
- [21] J. M. Tonnerre *et al.*, *Phys. Rev. Lett.* **75**, 740 (1995).
- [22] V. Chakarian *et al.*, *J. Magn. Magn. Mater.* **165**, 52 (1997).
- [23] Y. U. Idzerda *et al.*, *Synch. Radiat. News* **10**, 6 (1997).
- [24] J. F. Mackay *et al.*, *Phys. Rev. Lett.* **77**, 3925 (1996).
- [25] J. W. Freeland *et al.*, *J. Appl. Phys.* **83**, 6290 (1998).
- [26] Here we have ignored intradomain scattering or scattering from domain walls.
- [27] F. Scheurer *et al.*, *Surf. Sci. Lett.* **245**, L175 (1991).
- [28] S. Folsch *et al.*, *Phys. Rev. B* **57**, R4293 (1998).
- [29] Y. U. Idzerda *et al.*, *J. Appl. Phys.* **76**, 6525 (1994).
- [30] Domain correlations may occur for noninteracting films if growth nonuniformities propagate vertically through the structure, acting as magnetic domain nucleation sites.